

This discussion paper is/has been under review for the journal Atmospheric Chemistry and Physics (ACP). Please refer to the corresponding final paper in ACP if available.

Effects of dust aerosols on tropospheric chemistry during a typical pre-monsoon season dust storm in northern India

R. Kumar^{1,2}, M. C. Barth², S. Madronich², M. Naja³, G. R. Carmichael⁴,
G. G. Pfister², C. Knote², G. P. Brasseur^{1,5}, N. Ojha³, and T. Sarangi³

¹Advanced Study Program, National Center for Atmospheric Research, Boulder, CO, USA

²Atmospheric Chemistry Division, National Center for Atmospheric Research, Boulder, CO, USA

³Aryabhata Research Institute of Observational Sciences, Nainital, India

⁴Center for Global and Regional Environmental Research, University of Iowa, Iowa City, IA, USA

⁵Climate Service Center, Helmholtz Zentrum Geesthacht, Hamburg, Germany

Received: 25 October 2013 – Accepted: 24 December 2013 – Published: 14 January 2014

Correspondence to: R. Kumar (rkumar@ucar.edu)

Published by Copernicus Publications on behalf of the European Geosciences Union.

Title Page

Abstract

Introduction

Conclusions

References

Tables

Figures

◀

▶

◀

▶

Back

Close

Full Screen / Esc

Printer-friendly Version

Interactive Discussion



Abstract

This study examines the effect of a typical pre-monsoon season dust storm on tropospheric chemistry through a case study in northern India. Dust can alter photolysis rates by scattering and absorbing solar radiation, and provide surface area for heterogeneous reactions. We use the Weather Research and Forecasting model coupled with Chemistry (WRF-Chem) to simulate the dust storm that occurred during 17–22 April 2010 and investigate the contribution of different processes on mixing ratios of several key trace gases including ozone, nitrogen oxides, hydrogen oxides, methanol, acetic acid and formaldehyde. We revised the Fast Troposphere Ultraviolet Visible (F-TUV) photolysis scheme to include effects of dust aerosols on photolysis rates in a manner consistent with the calculations of aerosol optical properties for feedback to the meteorology radiation schemes. In addition, we added twelve heterogeneous reactions on the dust surface, for which six reactions have relative humidity dependent reactive uptake coefficients (γ). The inclusion of these processes in WRF-Chem is found to reduce difference between observed and modeled ozone from 16 ± 9 to 2 ± 8 ppbv and that in NO_y from 2129 ± 1425 to 372 ± 1225 pptv compared to measurements at the high altitude site Nainital in the central Himalayas, and reduce biases by up to 30 % in tropospheric column NO_2 compared to OMI retrievals. The simulated dust storm acted as a sink for all the trace gases examined here and significantly perturbed their spatial and vertical distributions. The reductions in these gases are estimated as 5–100 % and more than 80 % of this reduction was due to heterogeneous chemistry. The RH dependence of γ is also found to have substantial impact on the distribution of trace gases, with changes of up to 20–25 % in ozone and HO_2 , 50 % in H_2O_2 and 100 % in HNO_3 . A set of sensitivity analyses revealed that dust aging can reduce the uptake of trace gases (especially of H_2O_2 and acetic acid) by up to 50 % in dust source regions.

Dust aerosols and tropospheric chemistry

R. Kumar et al.

Title Page

Abstract

Introduction

Conclusions

References

Tables

Figures

◀

▶

◀

▶

Back

Close

Full Screen / Esc

Printer-friendly Version

Interactive Discussion



1 Introduction

Dust aerosols have gained considerable attention in the recent years not only because they constitute a major fraction of the particulate matter in the troposphere but also because they have important implications for air quality, visibility, the Earth's radiation budget (e.g. Haywood and Boucher, 2000; Seinfeld et al., 2004), biogeochemistry (e.g. Jickells et al., 2005), hydrological cycles (e.g. Miller et al., 2004; Zhao et al., 2011), and atmospheric chemistry (e.g. Dentener et al., 1996; Wang et al., 2012). The significance of dust aerosols for atmospheric chemistry has been manifested through several experimental (e.g. Goodman et al., 2000; Underwood et al., 2001; Li et al., 2006; Preszler Prince et al., 2007; Wagner et al., 2008; Cwiertny et al., 2008; Pradhan et al., 2010; Chen et al., 2011; Bedjanian et al., 2013a, b) and modeling studies (e.g. Zhang et al., 1994; Dentener et al., 1996; Zhang and Carmichael, 1999; Tang et al., 2004; Martin et al., 2003; Bauer et al., 2004; Tie et al., 2005; Hodzic et al., 2006; Zhu et al., 2010; Wang et al., 2012) during the past two decades.

Dust aerosols can influence atmospheric chemistry by affecting the photolysis rate coefficients through interaction with incoming solar radiation and by providing surface area for heterogeneous chemistry and deposition of different trace gases. It has been suggested that mineral dust aerosols are responsible for 5–20% reduction in photolysis rate coefficients of ozone and NO₂ throughout the Northern Hemisphere (e.g. Martin et al., 2003; Tie et al., 2005; Ying et al., 2011). These changes in photolysis rate coefficients then decrease the annual mean global concentration of OH by 9%, which in turn leads to increase in the concentrations of several volatile organic compounds (Martin et al., 2003). Heterogeneous reactions on dust surfaces generally reduce the concentration of key atmospheric trace gases such as ozone, nitrogen oxides, sulphur oxides and hydrogen oxides, but the amount of reported reduction in these gases varies widely, indicating that heterogeneous chemistry on dust surfaces is still not well understood. For example, the decreases in surface ozone are reported as 5–40% by different studies (Zhang et al., 1994; Dentener et al., 1996; Zhang and Carmichael, 1999;

ACPD

14, 1113–1158, 2014

Dust aerosols and tropospheric chemistry

R. Kumar et al.

Title Page

Abstract

Introduction

Conclusions

References

Tables

Figures

◀

▶

◀

▶

Back

Close

Full Screen / Esc

Printer-friendly Version

Interactive Discussion



Tang et al., 2004; Bauer et al., 2004; Zhu et al., 2010; Wang et al., 2012). Likewise, the decreases for sulphur dioxide, nitrogen oxides and hydrogen oxides are reported as 10–50 %, 16–100 % and 11–59 % respectively.

Even though this study is focused on the impact of heterogeneous processes on dust surfaces on the tropospheric chemistry in northern India, it is worth mentioning other implications of heterogeneous chemistry here. The heterogeneous uptake of trace gases can potentially affect the physiochemical properties of dust aerosols and enhance their ability to act as cloud condensation nuclei (CCN). Dust particles are generally hydrophobic when they are emitted but become hygroscopic as they travel in the atmosphere and become coated with nitrate, sulfate and organics (e.g. Levin et al., 1996; Kelly et al., 2007; Hatch et al., 2009). The coating process will also modify the distributions of dust as well as sulfate and nitrate aerosols, which in turn will increase the scattering of solar radiation by aerosols. The increase in size of dust particles due to coating will increase the probability of their removal from the atmosphere and such coated particles will experience less long range transport.

In general, box and regional modeling studies have focused mostly on heterogeneous chemistry on East Asian and Saharan dust aerosols, whereas there have been no such studies over the northern Indian region where dust storms occur frequently during the pre-monsoon (March, April, May; MAM) season (e.g. Prasad and Singh, 2007; Hegde et al., 2007). Global modeling studies have suggested that heterogeneous chemistry on dust aerosols can reduce surface ozone in northern India by 4–10 % (e.g. Dentener et al., 1996; Bauer et al., 2004). However, there has been a considerable improvement in our understanding of heterogeneous chemistry on dust aerosols since these global modeling studies were conducted. For example, experimental studies (e.g. Chen et al., 2011) have demonstrated that the uptake of gas-phase HNO_3 by dust particles is followed by release of gas-phase NO_x (both NO and NO_2) in the presence of broadband radiation. This process is known as the “renoxification” process

Dust aerosols and tropospheric chemistry

R. Kumar et al.

Title Page

Abstract

Introduction

Conclusions

References

Tables

Figures

◀

▶

◀

▶

Back

Close

Full Screen / Esc

Printer-friendly Version

Interactive Discussion



shown in Eq. (1)



where (g) and (a) represent the species in gas and adsorbed phase respectively. The relative humidity (RH) dependence of the reactive uptake coefficient for several species such as O₃ (Cwiertny et al., 2008), HNO₃ (Liu et al., 2008), OH (Bedjanian et al., 2013a), HO₂ (Bedjanian et al., 2013b), SO₂ (Preszler Prince et al., 2007) and H₂O₂ (Pradhan et al., 2010) has also been demonstrated. Therefore, it is essential to re-assess the importance of dust aerosols for tropospheric chemistry in northern India by taking into account these recent advancements.

In light of the above conditions, this manuscript examines the effects of dust aerosols on the distribution of many key trace gases including ozone, nitrogen oxides, hydrogen oxides, methanol, acetic acid and formaldehyde by incorporating the updated information on heterogeneous reactive uptake of trace gases in MOZCART chemical mechanism of Weather Research and Forecasting model coupled with Chemistry (WRF-Chem). We also revised the Fast Troposphere Ultraviolet Visible (F-TUV) scheme to include effects of dust aerosols on photolysis rates. This extended configuration of WRF-Chem is then used to simulate the impact of a typical pre-monsoon season dust storm on the regional tropospheric chemistry in northern India. This dust storm occurred during 17–22 April 2010 in northern India and a detailed analysis including evolution of this dust storm, dust emissions and its effects on local to regional scale aerosol optical properties and radiation budget are presented in a companion paper (Kumar et al., 2013).

The rest of the manuscript is organized as follows. Section 2 provides details of the WRF-Chem configuration used in this study along with the implementation of effect of dust aerosols on photolysis rates and heterogeneous chemistry on dust surfaces. This is followed by the description of observation site and measurement techniques used in this study (Sect. 3). Results from this study are presented in Sect. 4 and are summarized in Sect. 5.

Title Page

Abstract

Introduction

Conclusions

References

Tables

Figures

◀

▶

◀

▶

Back

Close

Full Screen / Esc

Printer-friendly Version

Interactive Discussion



2 The WRF-Chem Model

The version 3.4.1 of the Weather Research and Forecasting Model (Skamarock et al., 2008) coupled with Chemistry (Grell et al., 2005; Fast et al., 2006) is used here to simulate the distribution of trace species. The simulation domain is composed of 120×90×51 grid points in (x, y, z) direction with a horizontal resolution of 30 km×30 km extending in the vertical up to 10 hPa. Gas-phase chemistry is represented by the Model for Ozone and Related chemical Tracers, version 4 (MOZART-4, Emmons et al., 2010), and aerosol processes by the GOCART bulk aerosol scheme (Chin et al., 2002; Pfister et al., 2011). The dust emission scheme in the model is based on Ginoux et al. (2001) and calculates size resolved dust emissions online in five size bins ranging from 0.73–8.0 μm (effective radius) using the following equation:

$$F_p = \begin{cases} CSs_p u_{10m}^2 (u_{10m} - u_t) & \text{if } u_{10m} > u_t \\ 0 & \text{otherwise} \end{cases} \quad (2)$$

where F_p ($\text{kgm}^{-2}\text{s}^{-1}$) represents the emission flux for size bin p , C is an empirical proportionality constant ($\text{kgm}^{-5}\text{s}^2$), S is the source function representing the fraction of alluvium available for wind erosion, s_p is the fraction of each size class of dust in the emission, u_{10m} (ms^{-1}) is the horizontal wind speed at 10 m above the surface and u_t is the threshold velocity (ms^{-1}) below which dust emission does not occur and is a function of particle size, air density and surface moisture. The default value of C was proposed initially as $1 \times 10^{-9} \text{kgm}^{-5}\text{s}^2$ (Ginoux et al., 2001) but we have set it to $2.2 \times 10^{-8} \text{kgm}^{-5}\text{s}^2$ as the latter led to a good agreement between model and Aerosol Robotic Network (AERONET) measured aerosol optical depth and Angström exponent at seven sites in the model domain (Kumar et al., 2013). The simulations started on 10 April 2010 at 00:00 GMT and ended on 25 April 2010 at 18:00 GMT. The first three days of the model output are removed from the analysis to allow the model to spin up. Four dimensional data assimilation (FDDA) is applied to limit model errors in the

Title Page

Abstract

Introduction

Conclusions

References

Tables

Figures

◀

▶

◀

▶

Back

Close

Full Screen / Esc

Printer-friendly Version

Interactive Discussion



simulated meteorological fields (Lo et al., 2008). Further details regarding selection of the value for C , the simulation domain, geographical datasets, anthropogenic, biogenic, and biomass burning emissions, physical parameterizations, initial and lateral boundary conditions for meteorology and chemical fields, nudging coefficients and different emission inventories used in the model set-up are described in detail by Kumar et al. (2013).

2.1 Effect of aerosols on photolysis rates in WRF-Chem

In this study, we use the Fast-Troposphere Ultraviolet Visible (F-TUV) scheme to calculate photolysis rates for the MOZCART chemical mechanism. The F-TUV scheme is a simplified version of the National Center for Atmospheric Research's (NCAR) TUV model (Madronich and Weller, 1990) and was designed to reduce the computational costs associated with TUV (Tie et al., 2005). The F-TUV model utilizes the same physical processes as the TUV model except that the number of wavelengths in the TUV spectra (121–750 nm) was reduced from 140 to 17, making it eight times faster than the TUV model. The differences in the calculated photolysis rate coefficients between the TUV and F-TUV model are reported to be less than 5 % (Tie et al., 2005).

To include the effect of aerosols on photolysis rates, the F-TUV photolysis scheme in WRF-Chem calculates optical properties (optical depth, single scattering albedo and asymmetry parameter) for black carbon, organic carbon, sulphate and sea-salt aerosols, and passes them to a two-stream radiative transfer module where they interact with radiation to affect photolysis rate coefficients. These optical properties are also calculated in the aerosol optical driver of WRF-Chem and are used for feedback of aerosols on meteorology radiation schemes. Here, we make use of the optical driver calculated aerosol optical properties in F-TUV photolysis scheme to be consistent between the effects of aerosols on radiation and photolysis rate coefficients. This coupling automatically accounts for the effect of dust aerosols on photolysis rates in WRF-Chem, which was missing in the original F-TUV scheme. Further details regarding the coupling of the optical driver to the F-TUV photolysis scheme can be found in the Supplement.

Title Page

Abstract

Introduction

Conclusions

References

Tables

Figures

◀

▶

◀

▶

Back

Close

Full Screen / Esc

Printer-friendly Version

Interactive Discussion



2.2 Heterogeneous chemistry on dust surface in WRF-Chem

This study also extends the ability of the MOZCART chemical mechanism of WRF-Chem to simulate heterogeneous chemistry on the surface of dust particles by including 12 heterogeneous reactions listed in Table 1. The uptake of these gases on dust particles is assumed to be irreversible (Zhang and Carmichael, 1999). However, recent laboratory experiments have shown that the uptake of HNO_3 (Chen et al., 2011) is associated with release of gas phase NO_x , and those of OH (Bedjanian et al., 2013a) and HO_2 (Bedjanian et al., 2013b) are associated with the release of gas-phase H_2O_2 . The production of these gas phase species from heterogeneous chemistry is taken into account in this study. The production of NO_x from HNO_3 uptake is observed only in the presence of broadband irradiation with a yield of about 50 % (Chen et al., 2011), and thus the reaction of HNO_3 is set to yield 0.5 NO_2 during daytime in this study. The yields for H_2O_2 from reactions of OH and HO_2 with dust particles are reported to be 5 % (Bedjanian et al., 2013a) and 10 % (Bedjanian et al., 2013b) respectively and are set accordingly. These numbers differ from previous studies, which have assumed a 100 % conversion of HO_2 and 0 % conversion of OH into H_2O_2 (e.g. Zhu et al., 2010; Wang et al., 2012).

The pseudo first order reaction rate coefficient (s^{-1}) for the loss of a gas phase species g due to heterogeneous uptake by dust particles is calculated following Heikes and Thompson (1983) as:

$$k_g = \sum_{i=1}^5 \frac{4\pi r_i D_g V N_i}{1 + K_n[\chi + 4(1 - \gamma)/3\gamma]} \quad (3)$$

where $i = 1, 5$ represents five dust size bins used by the GOCART model, r_i and N_i represents the effective radius (cm) and number density (particles cm^{-3}) of particles in size bin i , V is the ventilation coefficient and taken as unity, D_g represents the gas-phase molecular diffusion coefficient of gas molecule g ($\text{cm}^2 \text{s}^{-1}$) and is calculated

Title Page

Abstract

Introduction

Conclusions

References

Tables

Figures

◀

▶

◀

▶

Back

Close

Full Screen / Esc

Printer-friendly Version

Interactive Discussion



following Jacobson (2005) as:

$$D_g = \frac{5}{16\rho_a A d_g^2} \sqrt{\left(\frac{m_a + m_g}{m_g}\right) \frac{RT m_a}{2\pi}} \quad (4)$$

where ρ_a is atmospheric mass density (g cm^{-3}), A is the Avogadro's number (6.022×10^{23} molecules mol^{-1}), d_g is the collision diameter (cm) of gas molecule g , R is the universal gas constant (8.31451×10^7 $\text{g cm}^2 \text{s}^{-2} \text{mol}^{-1} \text{K}^{-1}$), T is the absolute temperature (K), m_a (g mol^{-1}) and m_g (g mol^{-1}) are the molecular weights of air and gas respectively. In Eq. (5), K_n is the dimensionless Knudsen number defined as the ratio of the effective mean free path of a gas molecule in air (λ) to the effective particle radius r_i . χ represents a correction factor for anisotropic movement and is calculated as follow:

$$\chi = \frac{\left(\frac{4}{3}K_n + 0.71\right)}{K_n + 1} \quad (5)$$

WRF-Chem model simulates the mass mixing ratio (M_i in g g^{-1}) of dust particles, and the use of Eq. (5) requires the conversion of mass mixing ratios to the number concentration. This is performed using the following equation:

$$N_i = \frac{M_i \rho_a}{\left(\frac{4}{3}\pi r_i^3\right) \rho_p} \quad (6)$$

where ρ_p (g cm^{-3}) represents mass density of the dust particles and are taken as 2.5 and 2.65 g cm^{-3} to represent clay and silt in GOCART (Ginoux et al., 2001).

The reaction uptake coefficient γ is the most important parameter in the calculation of g , but the uncertainties in γ are very large and have been reported as more than three orders of magnitudes for certain species such as ozone and HNO_3 (Goodman et al.,

Title Page

Abstract

Introduction

Conclusions

References

Tables

Figures

◀

▶

◀

▶

Back

Close

Full Screen / Esc

Printer-friendly Version

Interactive Discussion



**Dust aerosols and
tropospheric
chemistry**

R. Kumar et al.

Title Page

Abstract

Introduction

Conclusions

References

Tables

Figures

◀

▶

◀

▶

Back

Close

Full Screen / Esc

Printer-friendly Version

Interactive Discussion

2000; Underwood et al., 2001; Michel et al., 2002). Such large uncertainties make the choice of γ very difficult. Since this study is focusing on Thar Desert dust aerosols for which information on heterogeneous chemistry kinetics is not available we use the best guess values reported for East Asian dust aerosols (Zhu et al., 2010) here for the γ values of dry dust particles except for OH and HO₂. The γ values for OH and H₂ are taken from Bedjanian et al. (2013a, b). The applied γ values for dry dust particles are shown in Table 1 and vary from 2.1×10^{-6} for NO₂ to 0.18 for OH. Further information about available measurements of γ for different species can be found in Zhu et al. (2010).

Many laboratory studies have also demonstrated the dependence of γ on relative humidity (RH), but such a RH dependence has generally been ignored in previous modeling studies (e.g. Dentener et al., 1996; Zhu et al., 2010; Wang et al., 2012). In this study, we include the RH dependence of γ for ozone (Cwiertny et al., 2008), HNO₃ (Liu et al., 2008), OH (Bedjanian et al., 2013a), HO₂ (Bedjanian et al., 2013b), H₂O₂ (Pradhan et al., 2010), and SO₂ (Preszler Prince et al., 2007). The variations of γ with relative humidity for different trace gases are shown in Fig. 1. The value of γ increases with RH for HNO₃, SO₂ and H₂O₂ while it decreases with RH for ozone, OH and HO₂. The rate coefficients, i.e., k_g values are estimated to be of the order of 10^{-3} – 10^{-5} s⁻¹ for OH, HO₂, H₂O₂, HNO₃, NO₃, N₂O₅ and CH₃COOH, and of the order of 10^{-7} – 10^{-8} s⁻¹ for ozone, NO₂, SO₂, CH₃OH and CH₂O.

The aging of dust particles through heterogeneous uptake of acidic gases and organic compounds is another important process that can influence the uptake of trace gases by dust particles. However, the dependence of k_g on aging of mineral dust aerosols is complex and not well understood. For example, the reactive uptake of ozone (Usher et al., 2003) on HNO₃ and SO₂ processed dust particles is reported to increase or decrease depending on the chemical nature of the particle, coverage of the coatings, as well as ambient RH. Due to the complexity of processes involved and lack of information on all 12 heterogeneous reactions, the effect of atmospheric processing of dust particles is not included in this study except for a set of sensitivity simulations con-

ducted to highlight the importance of this aging process. The treatment of dust aging for those sensitivity simulations is presented below.

2.3 Atmospheric aging/processing of dust particles

Laboratory experiments have shown that reactive uptake of ozone decreases by about 70 % on dust particles processed with HNO_3 (leading to nitrate coating) while it increases by about 33 % on dust particles processed with SO_2 as ozone reacts with surface bound sulfites/bisulfites to form sulfate (Usher et al., 2003). We have made an attempt here to simulate these changes in dust reactivity and quantify their impact on surface ozone. The simulation of these changes requires partitioning of fresh and aged dust particles and is done using the following procedure: in addition to total dust, two artificial dust tracers called “fresh_dust” and “aged_dust” are introduced into the model to keep track of fresh and aged dust particles. These tracers are included for all five size bins and thus we have a total of 10 tracers in the model. All these tracers undergo same transport and deposition processes as the original dust tracers.

The emission of fresh dust particles are set equal to the emission of total dust while the emissions of aged dust particles are set to zero. The initial and boundary conditions for fresh dust particles are set equal to those for total dust while those for aged dust particles are set to zero because the MOZART-4 output used for providing initial and boundary conditions does not include such a classification. The assumption that all dust particles entering into the model domain are fresh may introduce some uncertainty in the model results. However, such an uncertainty is anticipated to have a small contribution in the case presented here, as two model runs with and without including the regional dust emissions showed that most of the dust loading over the model domain came from emissions within the model domain during 17–22 April 2010.

The number concentration (particles cm^{-3}) of aged ($N_{a,i}$, $i = 1, 5$ represent five size bins) and fresh ($N_{f,i}$) dust particles is updated every time step as follows for each gas g considered: first, the number of molecules of gas g needed to completely coat one dust particle of a given size with a monolayer ($n_{\text{ml},g,i}$) is calculated as the ratio of sur-

Title Page

Abstract

Introduction

Conclusions

References

Tables

Figures

◀

▶

◀

▶

Back

Close

Full Screen / Esc

Printer-friendly Version

Interactive Discussion



[Title Page](#)[Abstract](#)[Introduction](#)[Conclusions](#)[References](#)[Tables](#)[Figures](#)[◀](#)[▶](#)[◀](#)[▶](#)[Back](#)[Close](#)[Full Screen / Esc](#)[Printer-friendly Version](#)[Interactive Discussion](#)

face area of the dust particle to the surface area occupied by a gas molecule. Second, the total number of gas molecules of g that can potentially adsorb to dust particles ($n_{\text{pot}, g, i}$) is calculated by multiplying k_g (s^{-1}) estimated in Eq. (5) with gas concentration (molecules cm^{-3}) and time step (180 s in this case). The ratio $n_{\text{pot}, g, i}/n_{\text{ml}, g, i}$ then provides the number concentration increment $\Delta_{a, g, i}$ of dust particles that could have aged (i. e. been completely coated with a monolayer of g) during this time step (180 s here). The sum of the increments $\Delta_{a, g, i}$ due to all gases considered in coating gives the total increment in aged particles $\Delta_{a, i}$. $\Delta_{a, i}$ is then subtracted from the number concentration of fresh dust particles $N_{f, i}$ and added accordingly to the number concentration of aged particles $N_{a, i}$.

The reactions of HNO_3 , NO_2 , NO_3 and N_2O_5 with dust particles are assumed to coat dust particles with nitrate and that of SO_2 is assumed to coat them with sulfate. All gases are given equal probability to react with dust particles, and in case the number concentration of fresh dust particles is limiting, then $\Delta_{a, i} > N_{f, i}$, which would lead to negative number concentrations of $N_{f, i}$. To overcome this problem, $N_{a, i}$ and $N_{f, i}$ are set to $N_{f, i}$ and zero respectively. This approach leads to mass conservation of tracers, and the sum of fresh and aged dust particle concentrations is always equal to the total dust number concentration. Both fresh and coated dust particle then react separately with trace gases.

2.4 Simulations conducted

A total of nine simulations were conducted (Table 2) to examine the impact of the dust storm on tropospheric chemistry. No_Dust serves as a base simulation in which heterogeneous chemistry on dust surface and effect of dust on photolysis rates are not included. Dust_J simulation includes the effect of dust aerosols on photolysis rates, while Dust_JH simulation is same as Dust_J but with addition of heterogeneous chemistry on dust surface taking into account the RH dependence of γ and renoxification process. Dust_JH_NoRH simulation is same as Dust_JH except that it does not in-

clude RH dependence of γ . In Dust_JH_NoReNO_x, the release of gas-phase NO₂ associated with uptake of HNO₃ is not considered to assess the importance of renoxification process. Dust_JH_NO₃ and Dust_JH_SO₄ simulations are designed to examine the influences of dust coated with nitrate and sulfate separately on uptake of ozone.

In these simulations, the uptake coefficient γ for aged dust particles is reduced by 70 % in Dust_JH_NO₃ and is increased by 33 % in Dust_JH_SO₄ (Usher et al., 2003). Dust particles are coated with both sulfate and nitrate in Dust_JH_NO₃_SO₄ to examine the combined effect of nitrate and sulfate coating on ozone uptake. Dust_JH_Sat is a hypothetical simulation where we assume that the presence of nitrate or sulfate monolayer on dust particle would saturate the dust particles and deactivate them for further catalytic uptake of O₃, OH, HO₂, H₂O₂, CH₃COOH, CH₃OH and HCHO, but the coating is assumed to have no effect on the uptake of HNO₃, NO₂, NO₃, N₂O₅ and SO₂. This comparison of Dust_JH_Sat with Dust_JH and Dust_J would provide bounds of the heterogeneous chemistry induced changes in tropospheric chemistry.

3 Observation datasets

3.1 Surface observations

This study uses surface ozone and NO_y (sum of nitrogen oxides) observations made at the high altitude site Nainital (79.45° E, 29.36° N, 1958 m a.m.s.l.) located in the central Himalayas. The observation site is bounded by high altitude (2–5 km) mountains in the north and east directions and opens to the Indo-Gangetic Plain region in the south and west directions. There are no major anthropogenic sources near Nainital and thus the observations at this site are envisaged to be representative of northern India (Kumar et al., 2010). Further details regarding the orography, vegetation cover, meteorological and chemical characteristics of Nainital can be found elsewhere (e.g. Sagar et al., 2004; Pant et al., 2006; Kumar et al., 2010; Sarangi et al., 2014). Ozone measurements are made using a standard ultraviolet absorption based instru-

Title Page

Abstract

Introduction

Conclusions

References

Tables

Figures

◀

▶

◀

▶

Back

Close

Full Screen / Esc

Printer-friendly Version

Interactive Discussion



ment, and NO_y measurements are made with a chemiluminescence-based instrument. More details about the measurement set-up, operating principle, accuracy, detection limits and calibration procedure are discussed elsewhere (e.g. Kumar et al., 2010; Sarangi et al., 2014). The model results are also compared with Aerosol Robotic Network (AERONET) measurements at seven sites in the model domain. Further details of AERONET and these observations sites can be found in Kumar et al. (2013).

3.2 Ozone Monitoring Instrument (OMI)

The Ozone Monitoring Instrument (OMI), aboard NASA's Earth Observing System (EOS) Aura satellite, measures the radiation backscattered by the Earth's atmosphere and surface over the 0.27–0.5 μm wavelength range with a spatial resolution of about 13 km \times 24 km at nadir in normal operational mode. These measured radiances are used for daily global retrievals of several trace species, such as ozone, NO_2 , BrO, SO_2 , formaldehyde and aerosols. Here, we use Level-2 tropospheric column NO_2 datasets made available by KNMI (Royal Netherlands Meteorological Institute) as they provide access to the averaging kernel and a priori profiles, which are needed to make a proper comparison between model profiles and satellite retrievals (e.g. Emmons et al., 2004). More details on the algorithm used to retrieve the tropospheric column NO_2 abundances at KNMI are described by Bucsele et al. (2006). These OMI NO_2 retrievals were found to correlate well with aircraft measurements made during the INTEX-B campaign (Boersma et al., 2008) and MAX-DOAS ground-based measurements (Kramer et al., 2008) but are also suggested to be biased positively by about 0–30 %, irrespective of season (e.g. Boersma et al., 2009a; Zhou et al., 2009).

To compare WRF-Chem results with OMI, the best quality OMI retrievals are used by reducing influence of clouds on OMI retrievals through selection of pixels with cloud fraction less than 0.3 and removing unreliable retrievals associated with a tropospheric column flag of greater than 0 (Boersma et al., 2009b). The nighttime pixels from OMI are also excluded for the comparison. These best quality retrievals are co-located in space and time with model output. The co-located WRF-Chem profiles are then trans-

Title Page

Abstract

Introduction

Conclusions

References

Tables

Figures

◀

▶

◀

▶

Back

Close

Full Screen / Esc

Printer-friendly Version

Interactive Discussion



formed using the averaging kernel and a priori profiles used in the satellite retrievals to obtain a model profile that OMI would measure for the modeled state of the atmosphere in the absence of other errors. More details about the method of model-OMI data co-location and convolution of model profiles with averaging kernel and a priori files can be found in Kumar et al. (2012).

4 Results and discussion

4.1 Model Evaluation

Kumar et al. (2013) present a detailed evaluation of simulated aerosol optical properties and here, we present a summary. The simulated aerosol optical depth (AOD), Angström exponent and single scattering albedo are compared against Aerosol Robotic Network (AERONET) measurements at seven sites in the model domain. It is found that the model generally underestimates the AOD over the model domain but is able to capture the temporal variations ($r = 0.5\text{--}0.88$) seen in AERONET measurements. The good agreement between modeled and AERONET observed Angström exponent indicates that the model is able to capture dust storm-induced variations in aerosol size. The comparison of model results with Moderate Resolution Imaging Spectroradiometer (MODIS) AOD retrievals shows that the model is also able to capture the spatial pattern of dust storm induced changes in the MODIS AOD as well as the spatial pattern of the dust plume. The average MODIS and WRF-Chem AOD (550 nm) values in high dust laden region are estimated as 0.80 ± 0.30 and 0.68 ± 0.28 respectively.

The variations in observed and WRF-Chem simulated (No_Dust, Dust_J, Dust_JH_NoRH and DUST_JH) daily average ozone and NO_y at Nainital during 13–24 April 2010 are shown in Fig. 2. The modeled time series of relative humidity and dust mass concentration for particles of 0.73, 1.4 and 8.0 μm effective radii at Nainital are also shown. Note that the WRF-Chem model at the resolution (30 km \times 30 km) used here is not able to capture the rapidly varying topography around Nainital and the alti-

Title Page

Abstract

Introduction

Conclusions

References

Tables

Figures

◀

▶

◀

▶

Back

Close

Full Screen / Esc

Printer-friendly Version

Interactive Discussion



the difference between average modeled and observed ozone from 16 ± 9 to 2 ± 8 ppbv and that in NO_y from 2102 ± 1425 to 346 ± 1225 pptv respectively.

The spatial distributions of average OMI retrieved and WRF-Chem (Dust_JH and No_Dust) simulated tropospheric column NO_2 during 13–16 April 2010 and 17–22 April 2010 are shown in Fig. 3. WRF-Chem profiles are convolved with OMI averaging kernels before comparison. The periods of 13–16 April 2010 and 17–22 April 2010 represent the periods of low and high dust emissions respectively over the model domain. The percentage differences in tropospheric column NO_2 between high and low dust emission periods are also shown for both OMI and WRF-Chem. Both the model and satellite data show similar spatial distributions with highest values along the Indo-Gangetic Plain region during both low and high dust emission periods, but WRF-Chem generally overestimates the OMI retrievals which is consistent with previous studies over the Indian region (Kumar et al., 2012; Ghude et al., 2013). However, the comparison between Dust_JH and No_Dust configurations of WRF-Chem shows that the inclusion of effects of dust aerosols improves the model performance and reduces the model bias with respect to OMI retrievals by up to 30 % especially in the Indo-Gangetic Plain region. The remaining bias in the model could be due to uncertainties in NO_x emission estimates in this region. The percentage difference plots show that WRF-Chem model is able to capture several features of changes in OMI retrieved spatial distribution of tropospheric column NO_2 between high and low dust emission periods. The domain averaged OMI and WRF-Chem (Dust_JH) tropospheric column NO_2 values over the geographical region ($70\text{--}80^\circ\text{E}$, $25\text{--}30^\circ\text{E}$) of maximum dust storm impact during low dust emission period are estimated as $(2.35 \pm 1.43) \times 10^{15}$ and $(3.95 \pm 2.43) \times 10^{15}$ molecules cm^{-2} respectively, and during high dust emission period are estimated as $(2.01 \pm 1.37) \times 10^{15}$ and $(3.41 \pm 2.80) \times 10^{15}$ molecules cm^{-2} respectively. The reduction in tropospheric column NO_2 during high dust emission period in both OMI and WRF-Chem indicates that the dust storm acted as a sink for NO_2 .

**Dust aerosols and
tropospheric
chemistry**

R. Kumar et al.

Title Page

Abstract

Introduction

Conclusions

References

Tables

Figures

◀

▶

◀

▶

Back

Close

Full Screen / Esc

Printer-friendly Version

Interactive Discussion



4.2 Impact of dust storm on photolysis rate coefficients

The impact of the dust storm on photolysis rates is examined by comparing the daytime (07:30–17:30 IST or 02:00–12:00 UTC) NO₂ photolysis rate coefficients calculated by the WRF-Chem model with Dust_J and No_Dust configurations (Fig. 4). The percentage difference between Dust_J and No_Dust configurations are also shown. NO₂ photolysis rates at the surface show a strong relationship with aerosol loading and are lowest over the Indo-Gangetic Plain region, which is where the anthropogenic emissions are stronger than those over other parts of the model domain. The inclusion of dust aerosols enhances the spatial heterogeneity of NO₂ photolysis rate and decreases it by 5–25 % over the Thar Desert and western Indo-Gangetic Plain region. The photolysis rate coefficients of other trace gases such as ozone, HNO₃, H₂O₂, CH₂O and N₂O₅ at the surface exhibit similar features (not shown) with decreases of the same order of magnitude. The magnitude of change in photolysis rates decreases with altitude and changes sign from negative to positive near 4 km because of the increase in actinic flux due to scattering of incoming solar radiation by dust aerosol layers underneath. The spatial structure of changes in photolysis rates at 100 hPa is similar to that at the surface with largest increases (1–5 %) over the Thar Desert and western Indo-Gangetic Plain region.

4.3 Impact of dust storm on trace gases at the surface

The spatial distributions of average surface ozone, SO₂, NO_x, HNO₃ and H₂O₂ simulated by WRF-Chem in Dust_JH and No_Dust during 17–22 April 2010 are compared in Fig. 5. Also shown are absolute total differences (Dust_JH - No_Dust) calculated using the Dust_JH simulation because this run led to the best agreement between model and observations at Nainital. Surface ozone shows a similar spatial distribution in both runs with lowest values over the Arabian Sea and highest values over the eastern Indo-Gangetic Plain region. However, the dust storm clearly leads to a reduction in ozone mixing ratios by 3–14 ppbv (5–25 %) over the Thar Desert and western Indo-

[Title Page](#)[Abstract](#)[Introduction](#)[Conclusions](#)[References](#)[Tables](#)[Figures](#)[◀](#)[▶](#)[◀](#)[▶](#)[Back](#)[Close](#)[Full Screen / Esc](#)[Printer-friendly Version](#)[Interactive Discussion](#)

Gangetic Plain region. The spatial distribution of reductions in ozone mixing ratios is consistent with the distribution of dust over the model domain and the amount of reduction is comparable to those reported by previous studies in dust source regions (e.g. Dentener et al., 1996; Tang et al., 2004; Pozzoli et al., 2008; Wang et al., 2012).

5 SO_2 and NO_x mixing ratios are highest along the Indo-Gangetic Plain region due to higher emissions in this region. Changes in SO_2 mixing ratios show a mixed response to heterogeneous chemistry with a decrease of 0.1–0.2 ppbv (8–10 %) over the Thar Desert region and an increase of 0.2–0.5 ppbv (2–6 %) over the eastern Indo-Gangetic Plain region. This is because the heterogeneous chemistry reduces SO_2 through reaction with dust particles while increases it through reduction of OH mixing ratios ($\text{SO}_2 + \text{OH} \rightarrow \text{Sulfate}$). The sign of the changes in SO_2 is thus determined by competition between these two reactions. In general, NO_x mixing ratios show a reduction of up to 0.5 ppbv (< 10 %) along the Indo-Gangetic Plain region and 0.2–0.3 ppbv (10–20 %) over the Thar Desert due to uptake of NO_2 by dust particles. The changes in NO_2 are also determined by the competition between the reactions of NO_2 with dust and OH where the former tends to decrease NO_2 while the latter tends to increase NO_2 due to reduced OH. The reduction in NO_x is in contrast with the results of Wang et al. (2012) who reported an increase in NO_x in the dust source region and attributed the increase to the renoxification process. Our study differs because Wang et al. (2012) assumed that renoxification process is active all the time, whereas this process is active only during daytime in our simulations. To quantify the contribution of renoxification process in NO_x budget, we compared the NO_x distributions simulated by Dust_JH and Dust_JH_NoReNOx configurations. The comparison (not shown) showed that the renoxification process does increase NO_x mixing ratios, but the magnitude of this increase (0.1–0.2 ppbv) is less likely than the reduction due to heterogeneous chemistry.

25 The spatial distributions of HNO_3 and H_2O_2 are largely modified by the dust storm with reduction of up to 2 ppbv ($\sim 99\%$). This is because these species are highly reactive with dust particles (Table 1). The large reduction in H_2O_2 mixing ratio estimated here is also in contrast with the results of Wang et al. (2012) who estimated an in-

**Dust aerosols and
tropospheric
chemistry**

R. Kumar et al.

Title Page

Abstract

Introduction

Conclusions

References

Tables

Figures

◀

▶

◀

▶

Back

Close

Full Screen / Esc

Printer-friendly Version

Interactive Discussion



crease in H_2O_2 . Wang et al. (2012) assumed a 100 % yield for the conversion of HO_2 into H_2O_2 through heterogeneous uptake, while we assume a yield of 10 % following recent work by Bedjanian et al. (2013b). NO_3 , N_2O_5 and CH_3COOH also show large reductions by Dust_JH with the highest decrease reaching up to 0.1 ppbv ($\sim 98\%$), 0.46 ppbv ($\sim 99\%$) and 0.45 ppbv ($\sim 96\%$) respectively. The uptake of HO_2 by dust particles leads to a maximum reduction of about 3.5 pptv ($\sim 40\%$) over the Thar Desert region, which is much less than those reported previously (e.g. Bian and Zender, 2003; Wang et al., 2012) and is attributed to use of a lower γ value in our study (< 0.064 vs. 0.1). The maximum reduction in OH, CH_2O and CH_3OH is estimated to be about 40 %, 21 % and 5 %, respectively.

The above discussion focuses only on the role of heterogeneous chemistry in changing the distribution of trace gases; however, these changes also include contributions from perturbations in photolysis rate coefficients. The individual contributions of heterogeneous chemistry and perturbation in photolysis rate coefficients to the total difference in distributions of trace gases at the surface are shown in Fig. 6. More than 80 % of the changes in distribution of these trace gases are explained by the heterogeneous chemistry. The changes in surface ozone induced by changed photolysis rate coefficients are within $\pm 1\text{--}3$ ppbv and are driven by the complex response of ozone to decreases in photolysis rate coefficients. A decrease in the photolysis rate coefficients leads to slower photochemical processing in general and thus decreased ozone production.

SO_2 and NO_x mixing ratios at the surface show an increase of up to 0.1 ppbv due to reduction in photolysis rate coefficients. The increase in NO_x and SO_2 is associated with a decrease in OH mixing ratios as reaction with OH is the main loss process for both NO_x and SO_2 . The decrease in ozone photolysis rate coefficient leads to a decrease of up to 30 % in OH ($\text{O}_3 + h\nu \rightarrow \text{O}^1\text{D} + \text{O}_2$, producing OH through reaction of O^1D with water vapour) mixing ratios. HNO_3 and H_2O_2 mixing ratios at the surface also show a small decrease of up to 0.4 and 0.6 ppbv in the Dust_J configuration relative to the No_Dust configuration. HNO_3 is produced mainly by the reaction of OH with NO_2

**Dust aerosols and
tropospheric
chemistry**

R. Kumar et al.

Title Page

Abstract

Introduction

Conclusions

References

Tables

Figures

◀

▶

◀

▶

Back

Close

Full Screen / Esc

Printer-friendly Version

Interactive Discussion



but the rate of change of HNO_3 is dominated by changes in OH as the reduction in OH (up to 30 %) is larger than that in NO_2 (up to 5 %). The reduction in H_2O_2 is also associated with reduction in OH and HO_2 mixing ratios. Since OH is the major oxidizing agent in the troposphere, a decrease in OH also leads to a decrease in the oxidizing capacity of the atmosphere and a consequent increase of up to 5–10 % in several trace gases such as CO, alkanes and alkenes at the surface.

4.4 Impact of dust storm on vertical distribution of trace gases

The vertical profiles of percentage total differences (Dust_JH – No_Dust) in average ozone, NO_x , HNO_3 , OH and BIGALK over the geographical region ($70\text{--}80^\circ\text{E}$, $25\text{--}30^\circ\text{N}$) of maximum dust influence are shown in Fig. 7, including the differences only due to heterogeneous chemistry (Dust_JH – Dust_J) and dust influence on photolysis rates (Dust_J – No_Dust). BIGALK represents alkanes with four or more carbon atoms in the MOZCART chemical mechanism and is shown to illustrate the dust storm induced changes in volatile organic compounds. The vertical distributions of average mass concentration for dust particles of $1.4\ \mu\text{m}$ effective radius and relative humidity are also shown to help the interpretation.

The changes in all the trace gases due to heterogeneous chemistry are much larger than those due to perturbations in photolysis rate coefficients, and are significant below 8 km, which is consistent with the vertical distribution of dust particles. All gases except BIGALK show a net reduction because of the larger changes induced by the heterogeneous chemistry. The reduction in OH due to decrease in ozone photolysis rate coefficient leads to a small increase of 1–4 % in NO_x . The reaction with OH is the only loss process for BIGALK and therefore BIGALK shows an increase due to both heterogeneous chemistry and perturbation in photolysis rates as both of these processes leads to a decrease in OH. The highest net decrease in ozone, NO_x , HNO_3 and OH are estimated as $\sim 16\%$, $\sim 26\%$, $\sim 91\%$ and $\sim 30\%$ respectively while the highest net increase in BIGALK is estimated as $\sim 26\%$. The vertical distribution of

[Title Page](#)[Abstract](#)[Introduction](#)[Conclusions](#)[References](#)[Tables](#)[Figures](#)[◀](#)[▶](#)[◀](#)[▶](#)[Back](#)[Close](#)[Full Screen / Esc](#)[Printer-friendly Version](#)[Interactive Discussion](#)

5 terminated by competition between the reactions of SO₂ with dust particles and OH. The reaction of SO₂ tries to reduce SO₂ due to increase in γ with RH while that with OH would decrease (increase) SO₂ if OH increases (decreases). The magnitudes of these RH induced changes in trace gases are comparable to those induced by heterogeneous chemistry (reported in Sect. 4.3). This suggests that consideration of RH dependent γ values in heterogeneous chemistry calculation is as important as is the accurate simulation of dust mass concentrations.

5 Impact of dust aging

10 The aging of dust particles through heterogeneous uptake of gases can modify the dust reactivity towards trace gases. We have made an attempt to simulate changes in the dust reactivity and uptake of trace gases due to nitrate and sulfate coating and the results are presented in this section. The spatial distributions of WRF-Chem simulated average mass concentration of fresh and aged dust particles of 1.4 μm effective radius at the surface in Dust_JH_N₃, Dust_JH_SO₄ and Dust_JH_NO₃_SO₄ configurations
15 during 17–22 April 2010 are shown in Fig. 10. The absolute changes in average surface ozone in these configurations relative to Dust_JH configuration are also shown. In general, fresh dust particles are seen mostly in and near the source regions because all dust particles are emitted as fresh and have much smaller concentration than the aged dust particles particularly outside the dust source regions. Among all the gases providing nitrate coating on dust particles, the HNO₃ uptake makes the highest contribution to the concentration of aged particles due to its higher mixing ratios and strong increase in its reactivity towards the dust surface with relative humidity. For example, if there are 10 fresh dust particles cm⁻³ of effective radius 0.73 μm , then the uptake of HNO₃, NO₂, NO₃ and N₂O₅ leads to about 2.5 aged dust particles cm⁻³ in one
20 time step (180 s) at RH = 0, and HNO₃ and NO₃ each provide about 1 dust particle. However, the number concentration of aged dust particles formed due to HNO₃ uptake increases to about 7 particles cm⁻³ per time step as RH increase to 20–40 %. The up-

Title Page

Abstract

Introduction

Conclusions

References

Tables

Figures

◀

▶

◀

▶

Back

Close

Full Screen / Esc

Printer-friendly Version

Interactive Discussion



**Dust aerosols and
tropospheric
chemistry**

R. Kumar et al.

Title Page

Abstract

Introduction

Conclusions

References

Tables

Figures

◀

▶

◀

▶

Back

Close

Full Screen / Esc

Printer-friendly Version

Interactive Discussion



take of SO_2 also increases with increase in relative humidity, but the SO_2 contribution to the aged particles is much less than that of HNO_3 due to lower SO_2 γ value. The decrease in ozone γ values for nitrate coated dust particles leads to an enhancement of 1–2 ppbv in surface ozone over the Thar Desert and western Indo-Gangetic Plain region relative to uncoated dust particles while increase in ozone γ values for sulfate coated dust particles leads to a reduction of 0.5–1 ppbv over these regions. Since nitrate coating leads to larger fraction of aged particles than the sulfate coating, surface ozone mixing ratios show an overall enhancement of up to 1 ppbv over the regions of high dust loadings when both sulfate and nitrate coated dust particles are allowed to react with ozone in the model.

The spatial distributions of lower and upper bounds for heterogeneous chemistry reaction rates induced changes in surface ozone, H_2O_2 , HCHO and CH_3COOH are shown in Fig. 11. Absolute mixing ratios of these gases in Dust_J configuration, in which dust aerosols affected photolysis rates only, are also shown to provide an idea of the modification in base levels of these gases due to heterogeneous chemistry. Lower and upper bounds for each gas are calculated by subtracting their average values in Dust_J configuration from those in Dust_JH and Dust_JH_Sat configurations respectively. As expected, the saturation of dust particles decreases the magnitude of reduction caused by heterogeneous chemistry for all the gases by 5–50%. The amount of maximum reduction in surface ozone changed from 20–25% to 15–20% when saturation effects are accounted for. The saturation of dust particles has a larger impact on the distribution of H_2O_2 and CH_3COOH as maximum reduction in both of these gases decreased to 20–40% (as compared to 70–90% for unsaturated dust particles) over the Thar Desert and dust source regions. Both of these gases show a small increase of 0.1–0.2 ppbv (less than 10%) outside the source regions for the case of saturated dust particles. The maximum reduction in HO_2 and OH (not shown) also changes from 20–40% in Dust_JH to 5–20% in Dust_JH_Sat. Some changes can also be discerned in the distribution of HCHO and CH_3OH (not shown) but they are within $\pm 5\%$.

5 tured the general features of the dust storm induced changes in spatial distribution of OMI retrieved tropospheric column NO_2 .

6 The dust storm leads to a decrease of 5–25 % in photolysis rate coefficients of ozone,
7 NO_2 and other trace gases at the surface and an increase of 1–5 % above 4 km. It is
8 found to have a significant impact on the regional tropospheric chemistry: a decrease
9 of 5–99 % is estimated in the mixing ratios of a variety of trace gases including ozone,
10 nitrogen oxides, hydrogen oxides, sulphur dioxide, methanol, acetic acid and formalde-
11 hyde at the surface. Analysis of the vertical distributions of these trace gases shows
12 that dust storm induced changes are significant up to an altitude 8 km and are esti-
13 mated as 80–90 % (5–10 times) for highly reactive gases such as HNO_3 , NO_3 , N_2O_5 ,
14 H_2O_2 and CH_3COOH . It is found that majority of these changes are induced by the het-
15 erogeneous chemistry, and the contribution of perturbation in photolysis rates generally
16 remained less than 10 %. An increase of up to 30 % in volatile organic compounds is
17 estimated due to decrease in OH concentrations.

18 The RH dependence of γ is found to play a large potential role in heterogeneous
19 chemistr. Sensitivity studies showed that the exclusion of the RH dependence can in-
20 troduce a difference of one-two orders of magnitude in heterogeneous reactions rate
21 constants, 20–25 % changes in ozone and HO_2 , and up to 50 % and 100 % changes in
22 H_2O_2 and HNO_3 , respectively. These effects are comparable to heterogeneous chem-
23 istry induced changes in these gases. We also tested the importance of atmospheric
24 aging of dust particles in the context of heterogeneous chemistry. Model experiments
25 based on laboratory studies of changes in dust reactivity due to atmospheric process-
ing showed that coating of dust with nitrate and sulfate may lead to changes of up
to 1 ppbv in surface ozone simulations. A hypothetical simulation is also conducted
by saturating the nitrate and sulfate coated dust particles for uptake of O_3 , HO_2 , OH,
 H_2O_2 , CH_3COOH , CH_3OH and HCHO. The saturation of dust particles is found to have
a larger impact on the distributions of H_2O_2 and CH_3COOH but a relatively small impact
on other gases.

**Dust aerosols and
tropospheric
chemistry**

R. Kumar et al.

Title Page

Abstract

Introduction

Conclusions

References

Tables

Figures

◀

▶

◀

▶

Back

Close

Full Screen / Esc

Printer-friendly Version

Interactive Discussion



**Dust aerosols and
tropospheric
chemistry**

R. Kumar et al.

Title Page

Abstract

Introduction

Conclusions

References

Tables

Figures

◀

▶

◀

▶

Back

Close

Full Screen / Esc

Printer-friendly Version

Interactive Discussion



This study clearly shows that the pre-monsoon season dust storm can potentially affect the regional tropospheric chemistry in northern India. However, the implications of the heterogeneous uptake of trace gases on aerosol size distributions and their feedbacks on radiation budget and cloudiness are not examined here. Dust particles coated with nitrate/sulfate may interact differently with radiation as compared to uncoated dust particles and can increase or decrease cloudiness depending upon their size distribution. Both of these processes will have important implications for the direct aerosol radiative forcing and the Elevated Heat Pump (EHP) hypothesis (Lau et al., 2006), which proposed that the absorption of solar radiation by dust and black carbon aerosols along the southern slopes of Himalayas modulates the meridional temperature gradient and leads to an early onset of Indian summer monsoon. The heterogeneous chemistry scheme implemented in the MOZCART chemical mechanism here can be easily extended to a more detailed aerosol module (e.g. MOSAIC) of WRF-Chem and these implications of heterogeneous chemistry for aerosols and their interaction with radiation and monsoon can be examined in a future study.

Nevertheless, this study demonstrates that the effects of dust aerosols through heterogeneous chemistry and perturbation in photolysis rates should be included in atmospheric chemistry transport models, especially for simulating air quality in northern India. At the same time, it is also imperative to improve the accuracy and precision of the reactive uptake coefficients, their dependence on relative humidity and atmospheric processing of dust particles. The impact of changes in the reactivity of aged dust for all the gases must be included in the models as they become available. In addition, co-located and extensive measurements of ozone and related gases, along with physical and chemical properties of dust aerosols in northern India are essential, especially during the dust storm season, for both model evaluation and to gain further insights into the effects of dust aerosols on tropospheric chemistry.

Supplementary material related to this article is available online at
[http://www.atmos-chem-phys-discuss.net/14/1113/2014/
acpd-14-1113-2014-supplement.pdf](http://www.atmos-chem-phys-discuss.net/14/1113/2014/acpd-14-1113-2014-supplement.pdf).

Acknowledgements. We thank L. Emmons and C. Wiedinmyer for their constructive suggestions on the manuscript. The datasets of initial and boundary conditions for meteorological fields were made available by the NCAR research data archive (<http://rda.ucar.edu/datasets/ds083.2/>). The datasets for initial and boundary conditions for chemical fields, biogenic emissions, biomass burning emissions, and programs used to process these data sets were made available by the NCAR Atmospheric Chemistry Division (<http://www.acd.ucar.edu/wrf-chem/>). We thank the OMI science team at KNMI for providing tropospheric NO₂ retrievals. The National Center for Atmospheric Research is supported by the National Science Foundation. Observations at Nainital are supported by ISRO-ATCTM project.

References

- Bauer, S. E., Balkanski, Y., Schulz, M., Hauglustaine, D. A., and Dentener, F.: Global modeling of heterogeneous chemistry on mineral aerosol surfaces: influence on tropospheric ozone chemistry and comparison to observations, *J. Geophys. Res.*, 109, D02304, doi:10.1029/2003JD003868, 2004.
- Bedjanian, Y., Romanias, M. N., and El Zein, A.: Interaction of OH radicals with Arizona test dust: uptake and products, *J. Phys. Chem. A*, 117, 393–400, doi:10.1021/jp311235h, 2013a.
- Bedjanian, Y., Romanias, M. N., and El Zein, A.: Uptake of HO₂ radicals on Arizona Test Dust, *Atmos. Chem. Phys.*, 13, 6461–6471, doi:10.5194/acp-13-6461-2013, 2013b.
- Bian, H. and Zender, C. S.: Mineral dust and global tropospheric chemistry: relative roles of photolysis and heterogeneous uptake, *J. Geophys. Res.*, 108, 4672, doi:10.1029/2002JD003143, 2003.
- Chen, H., Navea, J. G., Young, M. A., and Grassian, V. H.: Heterogeneous photochemistry of trace atmospheric gases with components of mineral dust aerosol, *J. Phys. Chem. A*, 115, 490–499, 2011.
- Chin, M., Ginoux, P., Kinne, S., Holben, B. N., Duncan, B. N., Martin, R. V., Logan, J. A., Higurashi, A., and Nakajima, T.: Tropospheric aerosol optical thickness from the GOCART model and comparisons with satellite and sunphotometer measurements, *J. Atmos. Sci.*, 59, 461–483, 2002.

**Dust aerosols and
tropospheric
chemistry**

R. Kumar et al.

Title Page

Abstract

Introduction

Conclusions

References

Tables

Figures

◀

▶

◀

▶

Back

Close

Full Screen / Esc

Printer-friendly Version

Interactive Discussion



Cwiertny, D. M., Young, M. A., and Grassian, V. H.: Chemistry and photochemistry of mineral dust aerosol, *Annu. Rev. Phys. Chem.*, 59, 27–51, doi:10.1146/annurev.physchem.59.032607.093630, 2008.

Dentener, F. J., Carmichael, G. R., Zhang, Y., Lelieveld, J., and Crutzen, P. J.: Role of mineral aerosol as a reactive surface in the global troposphere, *J. Geophys. Res.*, 101, 22869–22889, 1996.

Emmons, L. K., Walters, S., Hess, P. G., Lamarque, J.-F., Pfister, G. G., Fillmore, D., Granier, C., Guenther, A., Kinnison, D., Laepple, T., Orlando, J., Tie, X., Tyndall, G., Wiedinmyer, C., Baughcum, S. L., and Kloster, S.: Description and evaluation of the Model for Ozone and Related chemical Tracers, version 4 (MOZART-4), *Geosci. Model Dev.*, 3, 43–67, doi:10.5194/gmd-3-43-2010, 2010.

Fast, J. D., Gustafson Jr., W. I., Easter, R. C., Zaveri, R. A., Barnard, J. C., Chapman, E. G., and Grell, G. A.: Evolution of ozone, particulates, and aerosol direct forcing in an urban area using a new fully-coupled meteorology, chemistry, and aerosol model, *J. Geophys. Res.*, 111, D21305, doi:10.1029/2005JD006721, 2006.

Ganguly, D., Gadhavi, H., Jayaraman, A., Rajesh, T. A., and Misra, A.: Single scattering albedo of aerosols over the central India: Implications for the regional aerosol radiative forcing, *Geophys. Res. Lett.*, 32, L18803, doi:10.1029/2005GL023903, 2005.

Ghude, S. D., Pfister, G. G., Jena, C., van der A, R. J., Emmons, L. K., and Kumar, R.: Satellite constraints of nitrogen oxide (NO_x) emissions from India based on OMI observations and WRF-Chem simulations, *Geophys. Res. Lett.*, 40, 423–428, doi:10.1029/2012GL053926, 2012.

Ginoux, P., Chin, M., Tegen, I., Prospero, J. M., Holben, B., Dubovik, O., and Lin, S. J.: Sources and distributions of dust aerosols simulated with the GOCART model, *J. Geophys. Res.-Atmos.*, 106, 20255–20273, 2001.

Goodman, A. L., Underwood, G. M., and Grassian, V. H.: A laboratory study of the heterogeneous reaction of nitric acid on calcium carbonate particles, *J. Geophys. Res.*, 105, 29053–29064, 2000.

Grell, G. A., Peckham, S. E., Schmitz, R., McKeen, S. A., Frost, G., Skamarock, W. C., and Eder, B.: Fully coupled “online” chemistry within the WRF model, *Atmos. Environ.*, 39, 6957–6975, 2005.

**Dust aerosols and
tropospheric
chemistry**

R. Kumar et al.

Title Page

Abstract

Introduction

Conclusions

References

Tables

Figures

◀

▶

◀

▶

Back

Close

Full Screen / Esc

Printer-friendly Version

Interactive Discussion



- Hatch, D. C., Gierlus, K. M., Schuttelfeld, J. D., and Grassian, V. H.: Water adsorption and cloud condensation nuclei activity of calcite and calcite coated with model humic and fulvic acids, *Atmos. Environ.*, 42, 5672–5684, 2008.
- Haywood, J. and Boucher, O.: Estimates of the direct and indirect radiative forcing due to tropospheric aerosols: a review, *Rev. Geophys.*, 38, 513–543, 2000.
- Hegde, P., Pant, P., Naja, M., Dumka, U. C., and Sagar, R.: South Asian dust episode in June 2006: aerosol observations in the central Himalayas, *Geophys. Res. Lett.*, 34, L23802, doi:10.1029/2007GL030692, 2007.
- Heikes, B. G. and Thompson, A. M.: Effects of heterogeneous processes on NO_3 , HONO and HNO_3 chemistry in the troposphere, *J. Geophys. Res.*, 88, 10883–10895, 1983.
- Hodzic, A., Bessagnet, B., and Vautard, R.: A model evaluation of coarse-mode nitrate heterogeneous formation on dust particles, *Atmos. Environ.*, 40, 4158–4171, 2006.
- Jacobson, M. Z.: *Fundamentals of Atmospheric Modeling*, 2nd edn., Cambridge University Press, Cambridge, UK, 2005.
- Jickells, T. D., An, Z. S., Andersen, K. K., Baker, A. R., Bergametti, G., Brooks, N., Cao, J. J., Boyd, P. W., Duce, R. A., Hunter, K. A., Kawahata, H., Kubilay, N., laRoche, J., Liss, P. S., Mahowald, N., Prospero, J. M., Ridgwell, A. J., Tegen, I., and Torres, R.: Global iron connections between desert dust, ocean biogeochemistry and climate, *Science*, 308, 67–71, 2005.
- Kelly, J. T., Chuang, C. C., and Anthony, S. W.: Influence of dust composition on cloud droplet formation, *Atmos. Environ.*, 41, 2904–2904, 2007.
- Kleinman, L., Lee, Y.-N., Springston, S. R., Nunnermacker, L., Zhou, A., Brown, R., Hallock, K., Klotz, P., Leahy, D., Lee, J. H., Newman, L.: Ozone formation at a rural site in the southern United States, *J. Geophys. Res.*, 99, 3469–3482, 1994.
- Kumar, R., Naja, M., Venkataramani, S., and Wild, O.: Variations in surface ozone at Nainital, a high altitude site in the Central Himalayas, *J. Geophys. Res.*, 115, D16302, doi:10.1029/2009JD013715, 2010.
- Kumar, R., Naja, M., Pfister, G. G., Barth, M. C., Wiedinmyer, C., and Brasseur, G. P.: Simulations over South Asia using the Weather Research and Forecasting model with Chemistry (WRF-Chem): chemistry evaluation and initial results, *Geosci. Model Dev.*, 5, 619–648, doi:10.5194/gmd-5-619-2012, 2012.
- Kumar, R., Barth, M. C., Pfister, G. G., Naja, M., and Brasseur, G. P.: WRF-Chem simulations of a typical pre-monsoon dust storm in northern India: influences on aerosol optical properties

**Dust aerosols and
tropospheric
chemistry**

R. Kumar et al.

Title Page

Abstract

Introduction

Conclusions

References

Tables

Figures

◀

▶

◀

▶

Back

Close

Full Screen / Esc

Printer-friendly Version

Interactive Discussion



and radiation budget, *Atmos. Chem. Phys. Discuss.*, 13, 21837–21881, doi:10.5194/acpd-13-21837-2013, 2013.

Lau, K. M., Kim, M. K., and Kim, K. M.: Asian summer monsoon anomalies induced by aerosol direct forcing: the role of the Tibetan Plateau, *Clim. Dynam.*, 26, 855–864, doi:10.1007/s00382-006-0114-z, 2006.

Levin, Z., Ganor, E., and Gladstein, V.: The effects of desert particles coated with sulfate on rain formation in the eastern Mediterranean, *J. Appl. Meteorol.*, 35, 1511–1523, 1996.

Li, L., Chen, Z. M., Zhang, Y. H., Zhu, T., Li, J. L., and Ding, J.: Kinetics and mechanism of heterogeneous oxidation of sulfur dioxide by ozone on surface of calcium carbonate, *Atmos. Chem. Phys.*, 6, 2453–2464, doi:10.5194/acp-6-2453-2006, 2006.

Liu, Y., Gibson, E. R., Cain, J. P., Wang, H., Grassian, V. H., and Laskin, A.: Kinetic study of heterogeneous reactions of CaCO_3 particles with HNO_3 as a function of relative humidity using single particle analysis, *J. Phys. Chem. A*, 112, 1561–1571, 2008.

Madronich, S. and Weller, G.: Numerical integration errors in calculated tropospheric photodissociation rate coefficients, *J. Atmos. Chem.*, 10, 289–300, 1990.

Martin, R. V., Jacob, D. J., Yantosca, R. M., Chin, M., and Ginoux, P.: Global and regional decreases in tropospheric oxidants from photochemical effects of aerosols, *J. Geophys. Res.*, 108, 4097, doi:10.1029/2002JD002622, 2003.

Michel, A. E., Usher, C. R., and Grassian, V. H.: Heterogeneous and catalytic uptake of ozone on mineral oxides and dusts: a Knudsen cell investigation, *Geophys. Res. Lett.*, 29, 1665, doi:10.1029/2002GL014896, 2002.

Miller, R. L., Tegen, I., and Perlwitz, J.: Surface radiative forcing by soil dust aerosols and the hydrologic cycle, *J. Geophys. Res.*, 109, D04203, doi:10.1029/2003JD004085, 2004.

Pfister, G. G., Parrish, D. D., Worden, H., Emmons, L. K., Edwards, D. P., Wiedinmyer, C., Diskin, G. S., Huey, G., Oltmans, S. J., Thouret, V., Weinheimer, A., and Wisthaler, A.: Characterizing summertime chemical boundary conditions for air masses entering the US West Coast, *Atmos. Chem. Phys.*, 11, 1769–1790, doi:10.5194/acp-11-1769-2011, 2011.

Pozzoli, L., Bey, I., Rast, S., Schultz, M. G., Stier, P., and Feichter, J.: Trace gas and aerosol interactions in the fully coupled model of aerosol-chemistry-climate ECHAM5-HAMMOZ: 1. Model description and insights from the spring 2001 TRACE-P experiment, *J. Geophys. Res.*, 113, D07308, doi:10.1029/2007JD009007, 2008.

Pradhan, M., Kyriakou, G., Archibald, A. T., Papageorgiou, A. C., Kalberer, M., and Lambert, R. M.: Heterogeneous uptake of gaseous hydrogen peroxide by Gobi and Saharan

**Dust aerosols and
tropospheric
chemistry**

R. Kumar et al.

Title Page

Abstract

Introduction

Conclusions

References

Tables

Figures

◀

▶

◀

▶

Back

Close

Full Screen / Esc

Printer-friendly Version

Interactive Discussion

dust aerosols: a potential missing sink for H₂O₂ in the troposphere, *Atmos. Chem. Phys.*, 10, 7127–7136, doi:10.5194/acp-10-7127-2010, 2010.

Prasad, A. K. and Singh, R. P.: Changes in aerosol parameters during major dust storm events (2001–2005) over the Indo-Gangetic Plains using AERONET and MODIS data, *J. Geophys. Res.*, 112, D09208, doi:10.1029/2006JD007778, 2007.

Preszler Prince, A., Kleiber, P., Grassian, V. H., and Young, M. A.: Heterogeneous interactions of calcite aerosol with sulfur dioxide and sulfur dioxide nitric acid mixtures, *Phys. Chem. Chem. Phys.*, 9, 3432–3439, 2007.

Sarangi, T., Naja, M., Ojha, N., Kumar, R., Lal, S., Venkataramani, S., Kumar, A., Sagar, R., and Chandola, H. C.: First simultaneous measurements of ozone, CO and NO_y at a high altitude regional representative site in the central Himalayas, *J. Geophys. Res.*, doi:10.1022/2013JD020631, in press, 2014.

Seinfeld, J. H., Carmichael, G., Arimoto, R., Conant, W. C., Brechtel, F. J., Bates, T. S., Cahill, T. A., Clarke, A. D., Doherty, S. J., Flatau, F. J., Huebert, B. J., Kim, J., Markowicz, K. M., Quinn, P. K., Russell, L. M., Russell, P. B., Shimizu, A. Y., Song, C. H., TanShag, Y., Uno, I., Vogelmann, A. M., Weber, R. J., Woo, J., and Zhang, X. Y.: ACE-ASIA, Regional climatic and atmospheric chemical effects of Asian dust and pollution, *B. Am. Meteorol. Soc.*, 85, 367–380, 2004.

Skamarock, W. C., Klemp, J. B., Dudhia, J., Gill, D. O., Barker, D. M., Wang, W., and Powers, J. G.: A description of the advancedresearch WRF version 2, NCAR Tech. Note, NCAR/TN-468+STR, Natl. Cent. for Atmos. Res., Boulder, Colo, available at: <http://wrf-model.org/wrfadmin/publications.php> (10 January 2014), 2008.

Tang, Y., Carmichael, G. R., Kurata, G., Uno, I., Weber, R. J., Song, C.-H., Guttikunda, S. K., Woo, J.-H., Streets, D. G., Wei, C., Clarke, A. D., Huebert, B., and Anderson, T. L.: Impacts of dust on regional tropospheric chemistry during the ACE-Asia experiment: a model study with observations, *J. Geophys. Res.*, 109, D19S21, doi:10.1029/2003JD003806, 2004.

Tie, X., Madronich, S., Walters, S., Edwards, D. P., Ginoux, P., Mahowald, N., Zhang, R., Lou, C., and Brasseur, G.: Assessment of the global impact of aerosols on tropospheric oxidants, *J. Geophys. Res.*, 110, D03204, doi:10.1029/2004JD005359, 2005.

Underwood, G. M., Song, C. H., Phadnis, M., Carmichael, G. R., and Grassian, V. H.: Heterogeneous reactions of NO₂ and HNO₃ on oxides and mineral dust: a combined laboratory and modeling study, *J. Geophys. Res.*, 106, 18055–18066, 2001.

**Dust aerosols and
tropospheric
chemistry**

R. Kumar et al.

Title Page

Abstract

Introduction

Conclusions

References

Tables

Figures

◀

▶

◀

▶

Back

Close

Full Screen / Esc

Printer-friendly Version

Interactive Discussion



- Usher, C. R., Michel, A. E., Stec., D., and Grassian, V. H.: Laboratory studies of ozone uptake on processed mineral dust, *Atmos. Environ.*, 37, 5337–5347, 2003.
- Wagner, C., Hanisch, F., Holmes, N., de Coninck, H., Schuster, G., and Crowley, J. N.: The interaction of N_2O_5 with mineral dust: aerosol flow tube and Knudsen reactor studies, *Atmos. Chem. Phys.*, 8, 91–109, doi:10.5194/acp-8-91-2008, 2008.
- 5 Wang, K., Zhang, Y., Nenes, A., and Fountoukis, C.: Implementation of dust emission and chemistry into the Community Multiscale Air Quality modeling system and initial application to an Asian dust storm episode, *Atmos. Chem. Phys.*, 12, 10209–10237, doi:10.5194/acp-12-10209-2012, 2012.
- 10 Ying, Z., Tie, X., Madronich, S., Li, G., Massie, S.: Simulation of regional dust and its effect on photochemistry in the Mexico City area during MILAGRO experiment, *Atmos. Environ.*, 45, 2549–2558, 2011.
- Zhang, Y. and Carmichael, G. R.: The role of mineral aerosol in tropospheric chemistry in East Asia – a model study, *J. Appl. Meteorol.*, 38, 353–366, 1999.
- 15 Zhang, Y., Sunwoo, Y., Kotamarthi, V., and Carmichael, G. R.: Photochemical oxidant processes in the presence of dust: an evaluation of the impact of dust on particulate nitrate and ozone formation, *J. Appl. Meteorol.*, 33, 813–824, 1994.
- Zhao, C., Liu, X., Ruby Leung, L., and Hagos, S.: Radiative impact of mineral dust on monsoon precipitation variability over West Africa, *Atmos. Chem. Phys.*, 11, 1879–1893, doi:10.5194/acp-11-1879-2011, 2011.
- 20 Zhu, S., Butler, T., Sander, R., Ma, J., and Lawrence, M. G.: Impact of dust on tropospheric chemistry over polluted regions: a case study of the Beijing megacity, *Atmos. Chem. Phys.*, 10, 3855–3873, doi:10.5194/acp-10-3855-2010, 2010.

Dust aerosols and
tropospheric
chemistry

R. Kumar et al.

Table 1. The heterogeneous reactions and dry reactive uptake coefficients (γ_{dry}) used in this study are shown. The rightmost column shows the references based on which relative humidity dependence of γ_{dry} is specified.

Reaction	γ_{dry}	RH dependence
$\text{O}_3 + \text{Dust} \rightarrow \text{P}$	2.7×10^{-5}	Cwiertyny et al. (2008)
$\text{HNO}_3 + \text{Dust} \rightarrow 0.5\text{NO}_x + \text{P}$	2.0×10^{-3}	Liu et al. (2008)
$\text{NO}_2 + \text{Dust} \rightarrow \text{P}$	2.1×10^{-6}	–
$\text{NO}_3 + \text{Dust} \rightarrow \text{P}$	0.1	–
$\text{N}_2\text{O}_5 + \text{Dust} \rightarrow \text{P}$	0.03	–
$\text{OH} + \text{Dust} \rightarrow 0.05\text{H}_2\text{O}_2 + \text{P}$	0.18	Bedjanian et al. (2013a)
$\text{HO}_2 + \text{Dust} \rightarrow 0.1\text{H}_2\text{O}_2 + \text{P}$	6.42×10^{-2}	Bedjanian et al. (2013b)
$\text{H}_2\text{O}_2 + \text{Dust} \rightarrow \text{P}$	2×10^{-3}	Pradhan et al. (2010)
$\text{SO}_2 + \text{Dust} \rightarrow \text{P}$	3.0×10^{-5}	Preszler Prince et al. (2007)
$\text{CH}_3\text{COOH} + \text{Dust} \rightarrow \text{P}$	1×10^{-3}	–
$\text{CH}_3\text{OH} + \text{Dust} \rightarrow \text{P}$	1×10^{-5}	–
$\text{CH}_2\text{O} + \text{Dust} \rightarrow \text{P}$	1×10^{-5}	–

Title Page

Abstract

Introduction

Conclusions

References

Tables

Figures

◀

▶

◀

▶

Back

Close

Full Screen / Esc

Printer-friendly Version

Interactive Discussion



Dust aerosols and tropospheric chemistry

R. Kumar et al.

Title Page

Abstract

Introduction

Conclusions

References

Tables

Figures

◀

▶

◀

▶

Back

Close

Full Screen / Esc

Printer-friendly Version

Interactive Discussion

Table 2. Simulations designs used in this study and their purpose are shown.

Simulation Index	Model Configuration	Purpose
No_Dust	WRF-Chem without dust emissions but other aerosols affect photolysis rates	Serves as a base simulation
Dust_J	WRF-Chem with dust emissions and all aerosols affect photolysis rates	Comparison with No_Dust will quantify the effect of dust on photolysis rates and tropospheric chemistry
Dust_JH	Same as Dust_J but with heterogeneous chemistry considering RH dependence of γ and renoxification process included	Comparison with No_Dust will yield total impact of dust on tropospheric chemistry and comparison with DUST_J will yield contribution of heterogeneous chemistry
Dust_JH_NoRH	Same as Dust_JH but RH dependence of γ is not included	Comparison with Dust_JH will provide information on RH dependence of heterogeneous uptake of gases by dust
Dust_JH_NoReNOx	Same as Dust_JH but renoxification process is not included	Comparison with Dust_JH will provide contribution of renoxification process in NO_x budget.
Dust_JH_NO ₃	Same as Dust_JH but the effect of nitrate coated dust on uptake of ozone is included	Comparison with Dust_JH will provide information on changes in ozone uptake due to coating of dust with nitrate
Dust_JH_SO ₄	Same as Dust_JH but the effect of sulfate coated dust on uptake of ozone is included	Comparison with Dust_JH will provide information on changes in ozone uptake due to coating of dust with sulfate
Dust_JH_NO ₃ SO ₄	Same as Dust_JH but the effect of nitrate and sulfate coated dust on uptake of ozone is included	Comparison with Dust_JH will provide information on changes in ozone uptake due to coating of dust with nitrate and sulfate
Dust_JH_Sat	Same as Dust_JH but nitrate and sulfate coated particles are assumed to be saturated	Comparison with Dust_JH will provide upper limit on the effect of dust aging on the tropospheric chemistry

Dust aerosols and
tropospheric
chemistry

R. Kumar et al.

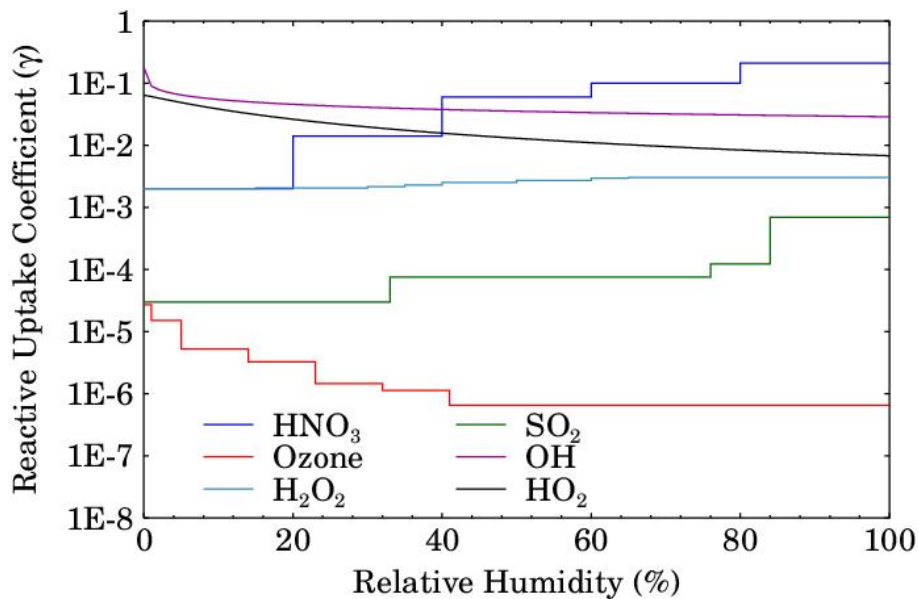


Fig. 1. The relative humidity dependence of reactive uptake coefficient (γ) for ozone, HNO_3 , OH, HO_2 , H_2O_2 and SO_2 used in this study.

Dust aerosols and
tropospheric
chemistry

R. Kumar et al.

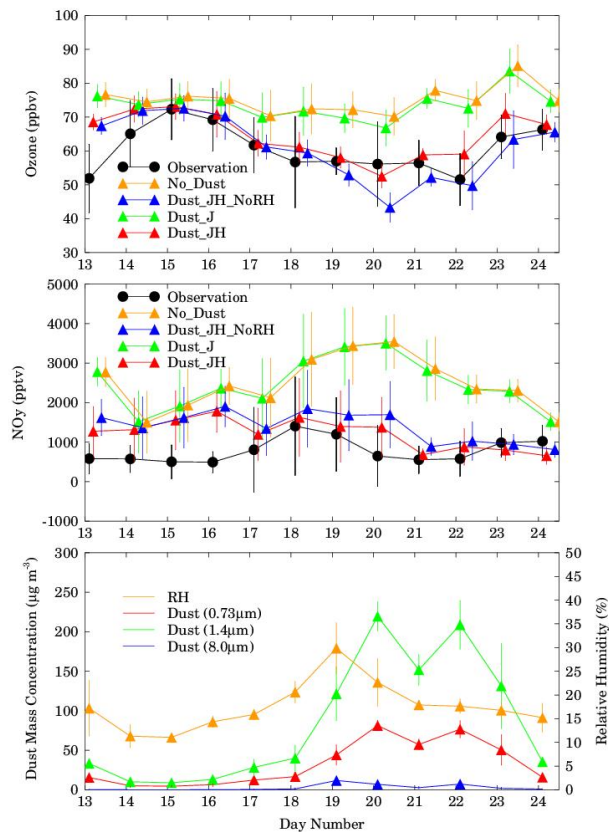


Fig. 2. Variations in observed and WRF-Chem simulated (No_Dust, Dust_JH_NoRH, Dust_J and Dust_JH) daily average ozone (top panel) and NO_y (middle panel) at Nainital during 13–24 April 2010. WRF-Chem simulated daily average mass concentration of dust particles of 0.73, 1.4 and 8.0 μm effective radii and relative humidity at Nainital are also shown. The vertical bars represent standard deviation in the average values.

[Title Page](#)[Abstract](#)[Introduction](#)[Conclusions](#)[References](#)[Tables](#)[Figures](#)[⏪](#)[⏩](#)[⏴](#)[⏵](#)[Back](#)[Close](#)[Full Screen / Esc](#)[Printer-friendly Version](#)[Interactive Discussion](#)

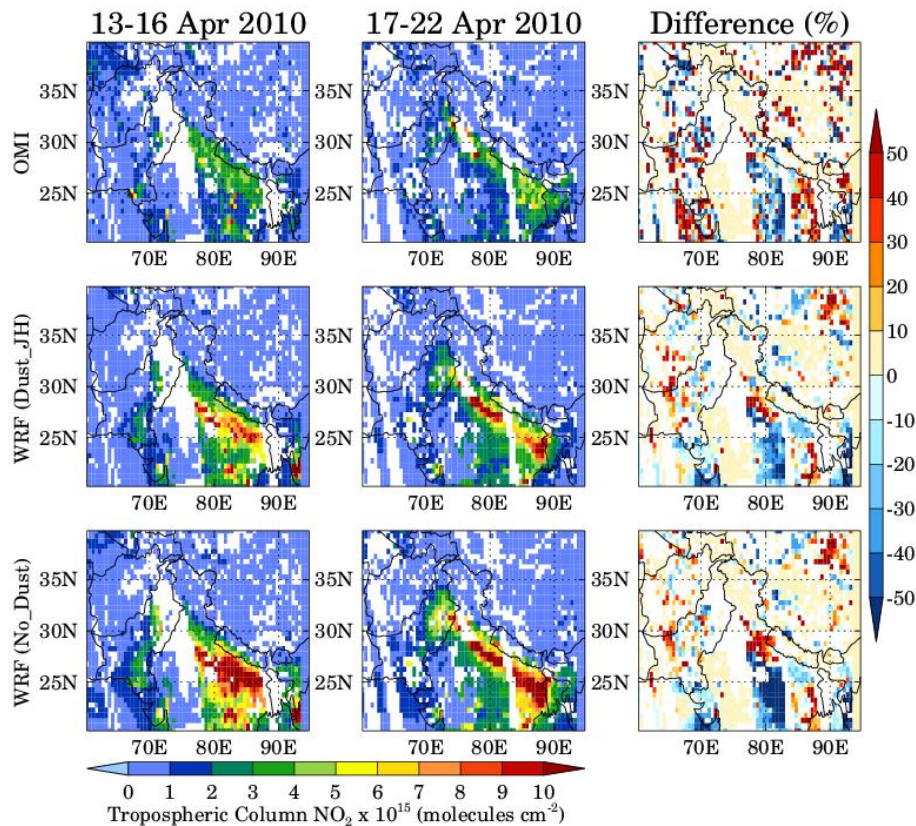


Fig. 3. Spatial distributions of OMI retrieved and WRF-Chem (Dust_JH and No_Dust) simulated tropospheric column NO_2 during the low (13–16 April 2010) and high (17–22 April 2010) dust emission periods. WRF-Chem profiles are convolved with OMI averaging kernels before comparison. The percentage differences between low and high dust emission periods are also shown.

Dust aerosols and tropospheric chemistry

R. Kumar et al.

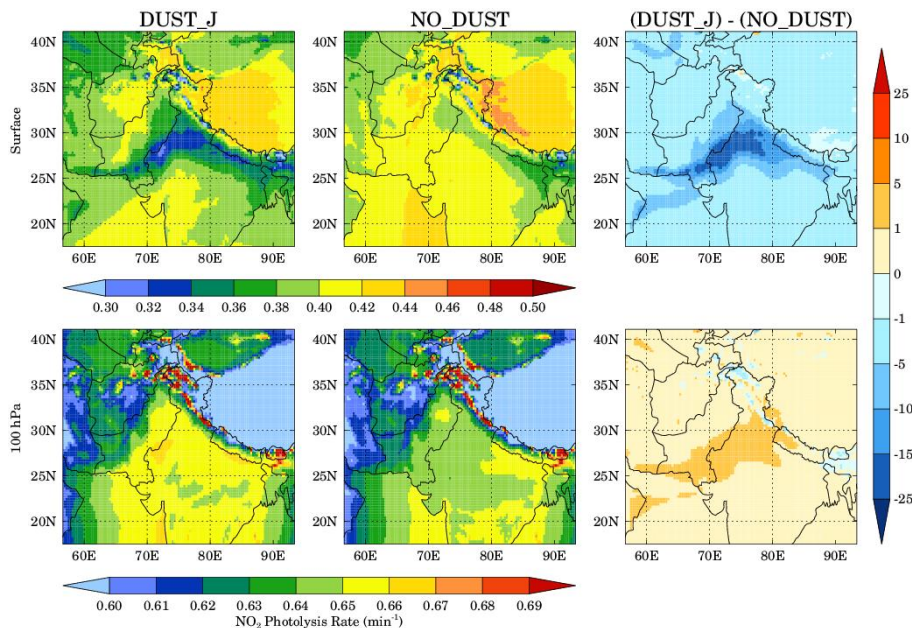


Fig. 4. Spatial distributions of the WRF-Chem simulated daytime (0200–1200 UTC) NO_2 photolysis rate with (Dust_J) and without dust (No_Dust) at the surface (top panel) and 100 hPa (bottom panel) during 17–22 April 2010 are shown. Percentage difference between Dust_J and No_Dust cases are also shown.

Dust aerosols and tropospheric chemistry

R. Kumar et al.

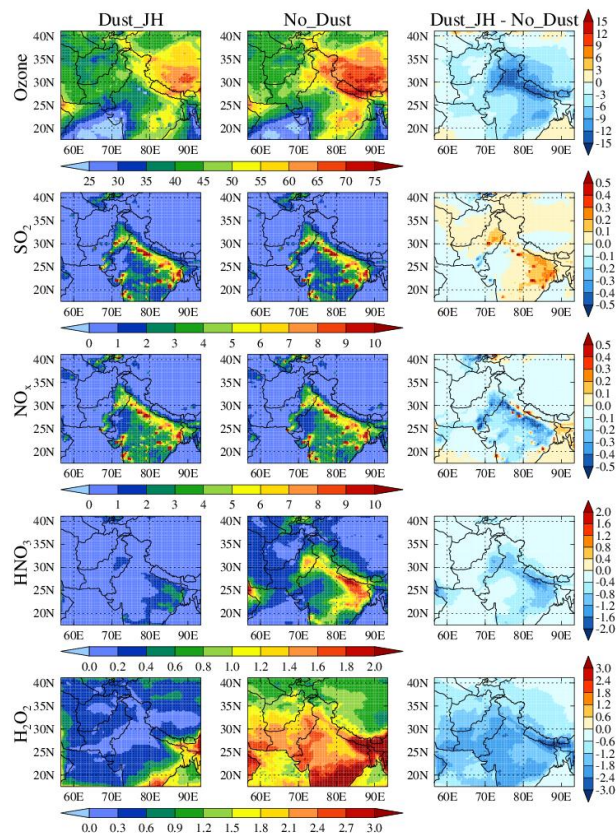


Fig. 5. Spatial distributions of average surface ozone, SO₂, NO_x, HNO₃ and H₂O₂ mixing ratios simulated by WRF-Chem with Dust_JH and No_Dust configuration during 17–22 April 2010. The absolute difference between the two configurations is also shown. All values are in ppbv.

Title Page

Abstract

Introduction

Conclusions

References

Tables

Figures

◀

▶

◀

▶

Back

Close

Full Screen / Esc

Printer-friendly Version

Interactive Discussion

Dust aerosols and
tropospheric
chemistry

R. Kumar et al.

Title Page

Abstract

Introduction

Conclusions

References

Tables

Figures

◀

▶

◀

▶

Back

Close

Full Screen / Esc

Printer-friendly Version

Interactive Discussion

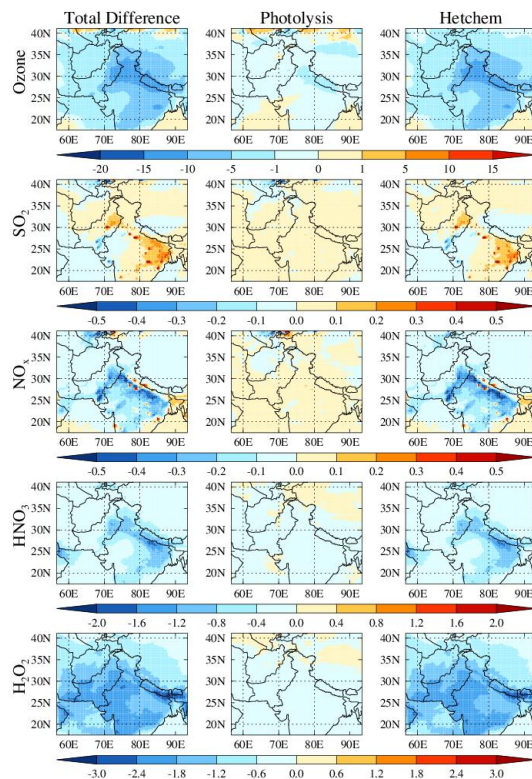


Fig. 6. Spatial distributions of absolute difference in average ozone, SO₂, NO_x, HNO₃ and H₂O₂ between Dust_JH and No_Dust (left panel), Dust_J and No_Dust representing the contribution of photolysis to total difference (middle panel), and Dust_JH and Dust_J representing the contribution of heterogeneous chemistry to total differences (right panel). All values are in ppb and for the surface layer of the model.

Dust aerosols and
tropospheric
chemistry

R. Kumar et al.

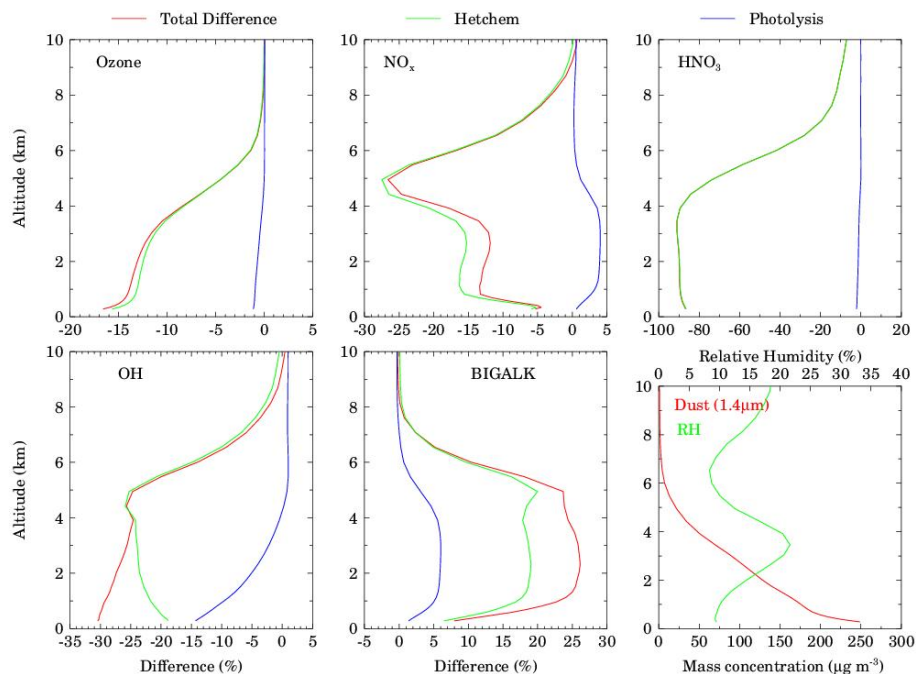


Fig. 7. Vertical profiles of percentage total difference (red lines) in average ozone, NO_x, HNO₃, OH and BIGALK between Dust_JH and No_Dust configuration over the geographical region (70–80° E, 25–30° N) of maximum dust influence. The contributions of heterogeneous chemistry (green lines) and photolysis (blue lines) to the total percentage difference are also shown. The vertical profiles of dust mass mixing ratios for particles of 1.4 μm effective radius and relative humidity are also shown to help interpretation.

Title Page

Abstract

Introduction

Conclusions

References

Tables

Figures

◀

▶

◀

▶

Back

Close

Full Screen / Esc

Printer-friendly Version

Interactive Discussion



Dust aerosols and tropospheric chemistry

R. Kumar et al.

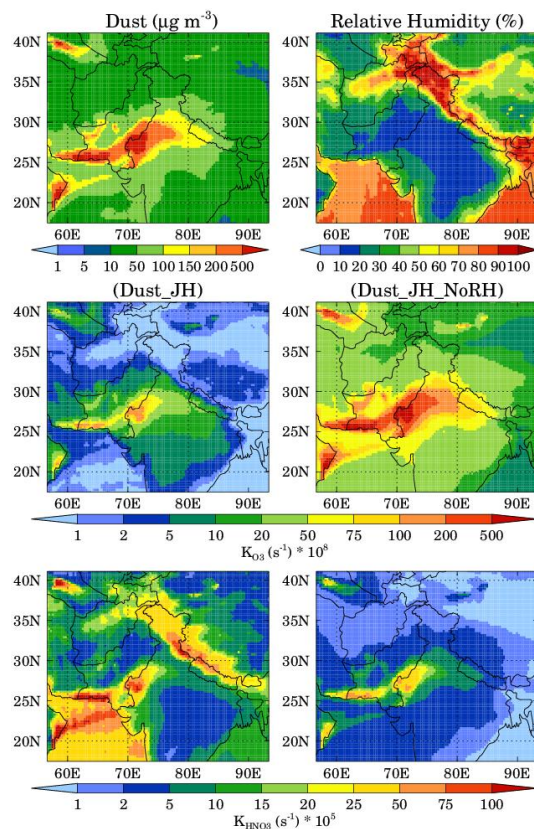


Fig. 8. Spatial distributions of average mass concentration for dust particles of $1.4 \mu\text{m}$ effective radius, relative humidity and pseudo first order rate coefficients for heterogeneous uptake of ozone (k_{O_3}) and HNO_3 (k_{HNO_3}) by dust particles in Dust_JH and Dust_JH_NoRH configurations during 17–22 April 2010.

Dust aerosols and
tropospheric
chemistry

R. Kumar et al.

Title Page

Abstract

Introduction

Conclusions

References

Tables

Figures

◀

▶

◀

▶

Back

Close

Full Screen / Esc

Printer-friendly Version

Interactive Discussion

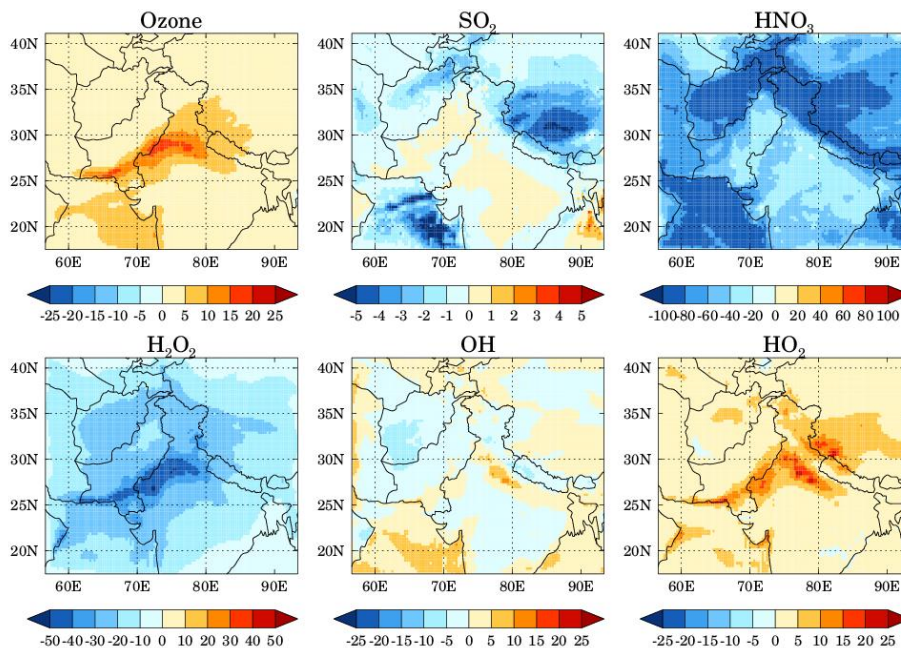


Fig. 9. Spatial distributions of relative percentage differences in ozone, SO_2 , HNO_3 , H_2O_2 , OH and HO_2 mixing ratios at the surface between Dust_JH and Dust_JH_NoRH configurations during 17–22 April 2010.

Title Page

Abstract

Introduction

Conclusions

References

Tables

Figures

◀

▶

◀

▶

Back

Close

Full Screen / Esc

Printer-friendly Version

Interactive Discussion

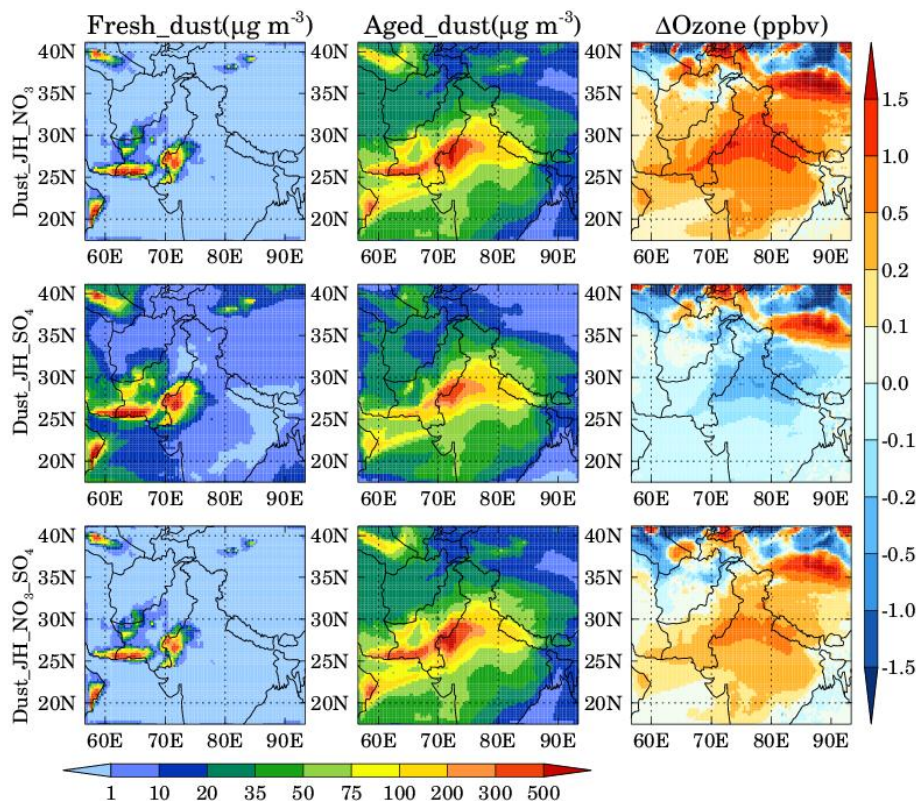


Fig. 10. Spatial distributions of WRF-Chem simulated average mass concentration of fresh and aged dust particles of $1.4 \mu\text{m}$ effective radius at the surface in Dust_JH_NO₃, Dust_JH_SO₄ and Dust_JH_NO₃_SO₄ configurations during 17–22 April 2010. ΔOzone is calculated by subtracting the average surface ozone in Dust_JH configuration from the corresponding average values in Dust_JH_NO₃, Dust_JH_SO₄ and Dust_JH_NO₃_SO₄ configurations respectively.

Dust aerosols and tropospheric chemistry

R. Kumar et al.

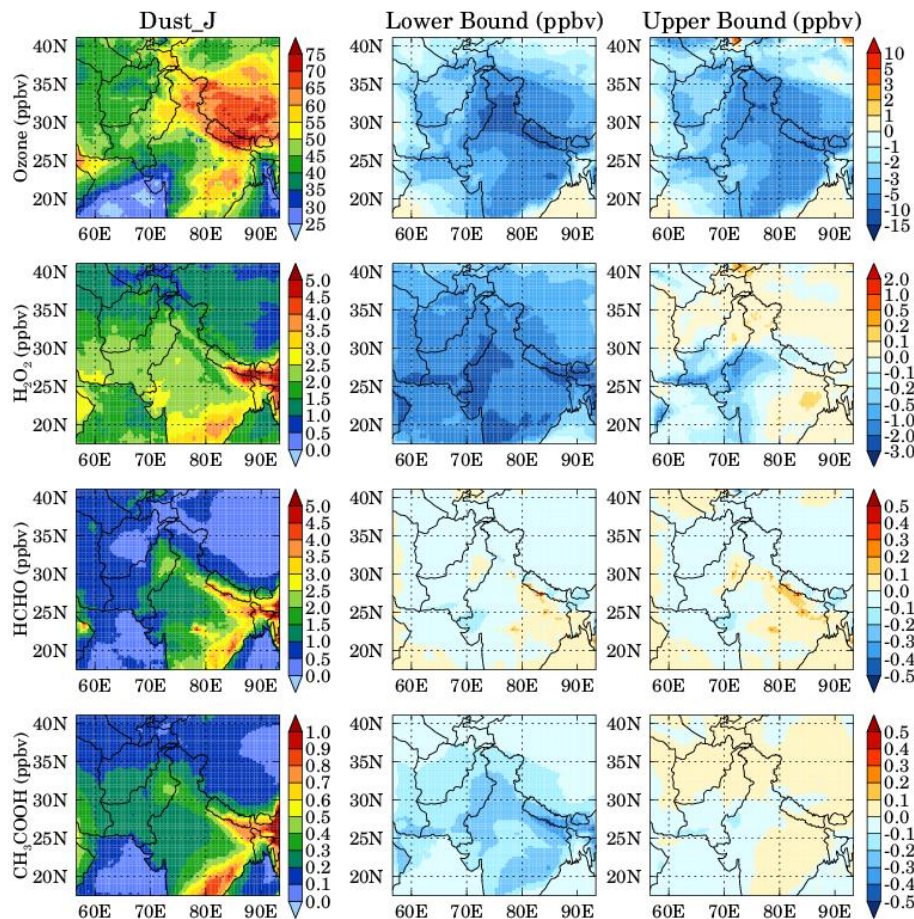


Fig. 11. Spatial distributions of average ozone, H_2O_2 , HCHO and CH_3COOH values at the surface in Dust_J configuration, and lower and upper bounds of heterogeneous chemistry induced changes in these gases during 17–22 April 2010.